JOINT BLIND DEBLURRING AND DESTRIPING FOR REMOTE SENSING IMAGES

Yi Chang, Houzhang Fang, Luxin Yan, and Hai Liu*

Science and Technology on Multi-spectral information Processing Laboratory, School of Automation, Huazhong University of Science and Technology, China.
{houzhangfang, yanluxin}@gmail.com

ABSTRACT

Deblurring and destriping are both classical problems for remote sensing images, which are known to be difficult. Treating deblurring and destriping separately, such a straightforward approach, however, suffers greatly from the defective output. This paper shows that the two problems can be successfully solved together and benefit greatly from each other within a unified variational framework. To do this, we propose a joint deblurring and destriping method by combining the framelet regularization and unidirectional total variation. Extensive experiments on simulation and real remote sensing images are carried out and the results of our joint model show significant improvement over conventional methods of treating the two tasks separately.

Index Terms—Blind image deblurring, destriping, total variation, tight frame, split Bregman method.

1. INTRODUCTION

The blur and stripes are common degradation problems in remote sensing images. Image blur could be the result of the atmospheric turbulence, scattering, and spacecraft motion, and the causes of the stripe issue include nonresponse of detector, relative gain and offset variations of detectors, and calibration errors. The blur and stripes severely limit the application of the resulting images. Therefore, many image deblurring [1]-[5] and destriping methods [6]-[9] have been proposed to improve the quality separately. Formally, the degraded process can be described as:

$$\mathbf{g} = \mathbf{H}\mathbf{f} + \mathbf{n}, \tag{1}$$

where $\mathbf{f} \in \mathbf{R}^N$ and $\mathbf{g} \in \mathbf{R}^N$ (N stands for the number of the image pixels.) represent the latent image and degraded image, respectively. $\mathbf{H} \in \mathbf{R}^{N\times N}$ denotes the matrix formed from the point spread function (PSF) $\mathbf{h}$. In this paper, $\mathbf{n} \in \mathbf{R}^N$ contain both stripe noise and random noise.

In conventional works, a nature solution to the blur and stripes would be handled one by one. However, if the destriping process is performed firstly, the strong edge structures belonging to the blur image would be unavoidably damaged, leading to the difficulty in estimating the accurate PSF in the blind image deblurring. Thus, the next blind image deblurring will be more difficult and will probably introduce unexpected artifacts. What is more, any residual stripes will be greatly aggravated by the blind image deblurring. On the contrary, if the blind image deblurring is accomplished firstly, the stripes will be easily regarded as the edges to be recovered so that the stripe artifacts will be much more severe. As a result, the removal of the stripe noise in the next would be much harder.

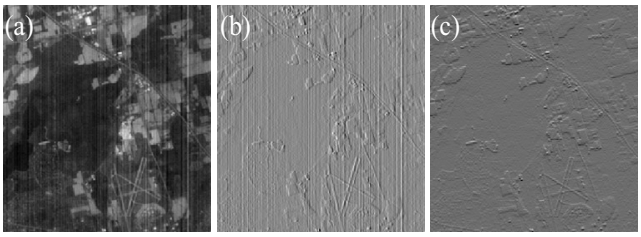

Fig. 1. (a) Original remote sensing image. (b) Horizontal derivative. (c) Vertical derivative.

In this paper, we present a joint deblurring and destriping method by combining the framelet regularization and unidirectional total variation (TV) to deblur and destripe simultaneously. With such a combination, the proposed method connects the deblurring and destriping in a unified framework by seeking the piecewise smooth solution iteratively. To the best of our knowledge, this is the first attempt to incorporate the two problems into a unified framework.

2. THE PROPOSED METHOD

2.1. Problem Formulation

In conventional restoration works, the noise $\mathbf{n}$ is often assumed as random noise. In reality, however, the remote sensing image includes both the random noise and stripe noise. Therefore, it is necessary to model the stripe noise into the minimization for reasonably estimating the

process. Formally, given the blurred and striped image **g**, the clear image **f** and PSF **h** are expected to be estimated:

$$\{\hat{\mathbf{f}},\hat{\mathbf{h}}\} = \arg\min_{\mathbf{f},\mathbf{h}} \Phi(\mathbf{Hf}-\mathbf{g}) + \lambda_f R_f(\mathbf{f}) + \lambda_h R_h(\mathbf{h}), \quad (2)$$

The stripe noise, which have significantly directional characteristic, is much different from the random noise. We observed that the stripes have little influence on the gradients along the stripe lines, while the gradients across the stripe lines are changed heavily. To illustrate this, in Fig. 1 we show the derivatives of the hyperspectral image along two directions. The stripes badly change the gradient across the stripe lines [Fig. 1(b)], while the gradient along the stripe lines are influenced slightly [Fig. 1(c)]. This significant characteristic of striping images motivates us:

1. Keep the gradients along the stripe in **Hf** as that of the degraded image **g**.
2. Penalize the gradients across the stripe lines.

Therefore, we propose to translate motivation 1 to the following data fidelity term:

$$\Phi(\mathbf{Hf}-\mathbf{g}) = \frac{1}{2}\|\mathbf{Hf}-\mathbf{g}\|_2^2 + \frac{\rho}{2}\|\nabla_x(\mathbf{Hf}-\mathbf{g})\|_2^2, \quad (3)$$

where ρ is the parameter that balances the two terms. In this work, we regard the direction along the stripe as x-axis and across the stripe as y-axis. The first term is the conventional reconstruction constrain. The second term aims at preserving the gradients along the stripe in **Hf** as that of the degraded image **g**. This is very reasonable since the stripes influence the gradient along the stripes slightly.

In image restoration, the sparsity based regularizations [4, 5] and TV based regularizations [1, 2, 8, 9] have been the popular choices of the regularization terms. In this paper, the framelet regularization and the unidirectional TV are coupled to connect the deblurring and destriping issue:

$$R_f(\mathbf{f}) = \|\mathbf{Wf}\|_1 + \tau\|\nabla_y\mathbf{f}\|_1, \quad (4)$$

where **W** is the framelet transform using filters of framelet system. The B-splines framelet [4] is used in our implementation. The interested readers can refer to [4] for more implementation details on the framelet transform. The functional (4) is intuitive. The sparsity framelet regularization term penalizes the number of the large framelet transform coefficients of the image **f** in the framelet domain, which could be viewed as penalizing the number of the pixels with large discontinuities. Thus, the resulting minimizer **f** tends to be a piecewise smooth solution. However, by only using the framelet regularization, the stripes will be easily regarded as the structural information to be enhanced, especially when the stripes are quite severe. The unidirectional TV penalizes the L1-norm of the gradient across the stripes so as to remove the stripe noise, which is the translation of the motivation 2. By balancing the sparsity prior $\|\mathbf{Wf}\|_1$ and the constraints across the stripes $\|\nabla_y\mathbf{f}\|_1$ using the parameter τ, the proposed regularization term (4) will yield a piecewise smooth and non-stripes image **f**.

To favor piecewise constant PSF with discontinuities, we regularize the PSF by the TV norm [1]. Thus the final energy functional about **f** is:

$$\min_{\mathbf{f},\mathbf{h}} \frac{1}{2}\|\mathbf{Hf}-\mathbf{g}\|_2^2 + \frac{\rho}{2}\|\nabla_x(\mathbf{Hf}-\mathbf{g})\|_2^2 + \lambda_1\|\mathbf{Wf}\|_1 + \lambda_2\|\nabla_y\mathbf{f}\|_1 + \lambda_3\|\nabla\mathbf{h}\|_1. \quad (5)$$

For convenience, we set the regularization parameters as λ_1, λ_2 and λ_3, respectively. Note that the proposed model is a general framework which can handle different kinds of blurs and stripes, e.g., out-of-focus blur, uniform blurs, non-periodical stripes, non-uniform stripes and etc.

2.2. Optimization

There are two unknowns of **h** and **f** to be estimated. The most commonly used approach is an alternative iteration scheme [4]. The alternative iteration scheme is described in two steps.

f-step: given the blur kernel, compute the clear image, i.e.,

$$\min_{\mathbf{f}} \frac{1}{2}\|\mathbf{Hf}-\mathbf{g}\|_2^2 + \frac{\rho}{2}\|\nabla_x(\mathbf{Hf}-\mathbf{g})\|_2^2 + \lambda_1\|\mathbf{Wf}\|_1 + \lambda_2\|\nabla_y\mathbf{f}\|_1. \quad (6)$$

h-step: given the clear image, compute the blur kernel, i.e.,

$$\min_{\mathbf{h}} \frac{1}{2}\|\mathbf{Hf}-\mathbf{g}\|_2^2 + \frac{\rho}{2}\|\nabla_x(\mathbf{Hf}-\mathbf{g})\|_2^2 + \lambda_3\|\nabla\mathbf{h}\|_1. \quad (7)$$

Because the L1-norm terms in (6) and (7) are nondifferentiable and nonseparable, it is a very challenging problem to find an efficient method to optimize the proposed model. To solve the minimizations involving such term, we introduce the split Bregman iteration [10].

In **f**-step, the basic idea of split Bregman iteration is to convert the unconstrained minimization problem on **f** in (6) into a constrained one by introducing auxiliary variables $\mathbf{d}_1 = \mathbf{Wf}$ and $\mathbf{d}_2 = \nabla_y\mathbf{f}$. Then, the problem could be further transformed into an unconstrained minimization with strictly enforcing the constraints by applying the Bregman iteration:

$$\begin{aligned}\min_{\mathbf{f},\mathbf{d}_1,\mathbf{d}_2} &\frac{1}{2}\|\mathbf{Hf}-\mathbf{g}\|_2^2 + \frac{\rho}{2}\|\nabla_x(\mathbf{Hf}-\mathbf{g})\|_2^2 + \lambda_1\|\mathbf{d}_1\|_1 + \lambda_2\|\mathbf{d}_2\|_1 \\ &+ \frac{\alpha}{2}\|\mathbf{d}_1-\mathbf{Wf}-\mathbf{b}_1\|_2^2 + \frac{\beta}{2}\|\mathbf{d}_2-\nabla_y\mathbf{f}-\mathbf{b}_2\|_2^2,\end{aligned} \quad (8)$$

where α, β are penalization parameters. Further, the functional (8) is converted into three separate subproblems.

- The **f**-related subproblem is

$$\begin{aligned}\min_{\mathbf{f}} &\frac{1}{2}\|\mathbf{H}^k\mathbf{f}-\mathbf{g}\|_2^2 + \frac{\rho}{2}\|\nabla_x(\mathbf{H}^k\mathbf{f}-\mathbf{g})\|_2^2 \\ &+ \frac{\alpha}{2}\|\mathbf{d}_1^k-\mathbf{Wf}-\mathbf{b}_1^k\|_2^2 + \frac{\beta}{2}\|\mathbf{d}_2^k-\nabla_y\mathbf{f}-\mathbf{b}_2^k\|_2^2.\end{aligned} \quad (9)$$

It is a least-square problem, which is equivalent to the following linear system:

$$\begin{aligned}&((\mathbf{H}^k)^T\mathbf{H}^k + \rho(\mathbf{H}^k)^T\nabla_x^T\nabla_x\mathbf{H}^k + \alpha\mathbf{W}^T\mathbf{W} + \beta\nabla_y^T\nabla_y)\mathbf{f}^{k+1} \\ &= (\mathbf{H}^k)^T\mathbf{g} + \rho(\mathbf{H}^k)^T\nabla_x^T\nabla_x\mathbf{g} + \alpha\mathbf{W}^T(\mathbf{d}_1^k-\mathbf{b}_1^k) + \beta\nabla_y^T(\mathbf{d}_2^k-\mathbf{b}_2^k).\end{aligned} \quad (10)$$

- The $\mathbf{d}_1$-related subproblem is:

$$\min_{\mathbf{d}_1} \lambda_1 \| \mathbf{d}_1 \|_1 + \frac{\alpha}{2} \| \mathbf{d}_1 - \mathbf{W}\mathbf{f}^{k+1} - \mathbf{b}_1^k \|_2^2 . \quad (11)$$

The subproblem in (11) could be solved by using a shrinkage operator in the following way:

$$\mathbf{d}_1^{k+1} = \text{shrink}(\mathbf{W}\mathbf{f}^{k+1} + \mathbf{b}_1^k, \frac{\lambda_1}{\alpha}), \quad (12)$$

where

$$\text{shrink}(r, \xi) = \frac{r}{|r|} * \max(r - \xi, 0). \quad (13)$$

Once $\mathbf{f}^{k+1}$ is obtained by (10), $\mathbf{d}_1$ and $\mathbf{d}_2$ can be computed parallelly. Thus, $\mathbf{d}_2$ could be expressed as:

$$\mathbf{d}_2^{k+1} = \text{shrink}(\nabla_y \mathbf{f}^{k+1} + \mathbf{b}_2^k, \frac{\lambda_2}{\beta}). \quad (14)$$

Finally, we update Bregman variables $\mathbf{b}_1$ and $\mathbf{b}_2$ as follows:

$$\begin{cases} \mathbf{b}_1^{k+1} = \mathbf{b}_1^k + (\mathbf{W}\mathbf{f}^{k+1} - \mathbf{d}_1^{k+1}), \\ \mathbf{b}_2^{k+1} = \mathbf{b}_2^k + (\nabla_y \mathbf{f}^{k+1} - \mathbf{d}_2^{k+1}). \end{cases} \quad (15)$$

In **h**-step, the split Bregman iteration is also employed to solve the PSF **h**. Similarly, the solution step of PSF **h** is similar to that of (9)-(10). In addition, we impose positive constraints on **f** and **h**, and the PSF is constrained to satisfy $\sum \mathbf{h}(i, j) = 1$ [1, 2].

3. EXPERIMENTAL RESULTS

We compared the proposed model with TV based deblurring algorithm [1] (TV), current Variational and Stationary Noise Remover destriping method [9] (VSNR), their combined method. If firstly remove the stripe noise by VSNR, then deblur the destriped results with TV, we mark the combined method as VSNR-TV, otherwise mark it TV-VSNR. The quantitative assessments were Peak Signal-to-Noise Ratio (PSNR), the universal image quality index (UIQI) [11] and the blind image quality index BIQI [12]. The larger PSNR and UIQI are, the better the restored image is. The smaller BIQI is, the better the image quality is.

In Fig. 2, we showed the restored results of different method. Fig. 2(a) is the original high-quality QuickBird remote sensing subimage of 256×256 pixels. We degraded Fig. 2(a) with a 5×5 Gaussian blur (standard deviation $\sigma = 2.1$) and additional stripe noise. With the TV method in Fig. 2(c), it is observed that most details are restored, but the stripes are aggravated. This is because the stripes are inevitably regarded as the edges to be recovered. In Fig. 2(d), it can be seen obviously that much residual stripes still exist. Such a result is not surprising as the stripes in Fig. 2(b) are badly aggravated, which highly increases the difficulty in removing the stripes. The VSNR-TV can easily remove all the stripes, while the piecewise constant effects are unexpectedly introduced, as

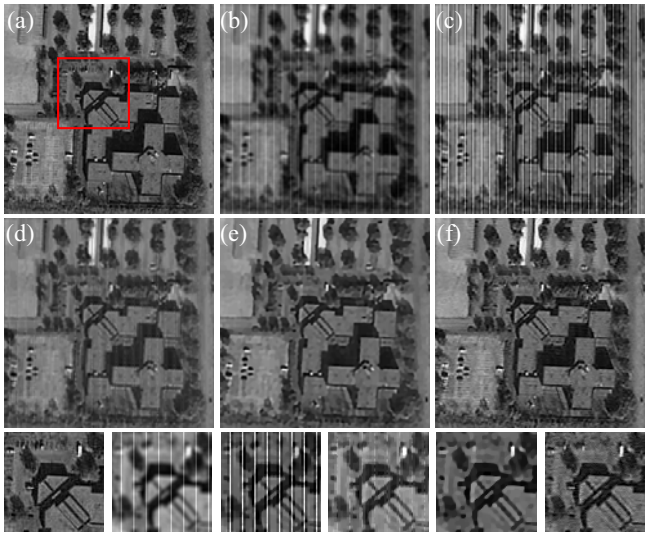

Fig. 2. Visual comparison by various methods. (a) Original clear image. (b) Blurred and striped image. Restored results by (c) TV. (d) TV-VSNR. (e) VSNR-TV. (f) Proposed method. The third row are the close-ups extracted from (a)-(f), respectively.

Table I
EVALUATION INDICES COMPARISONS OF DIFFERENT METHODS

Index	Degraded	TV-VSNR	VSNR-TV	Proposed
PSNR	21.71	21.96	24.94	**26.37**
UIQI	0.47	0.58	0.73	**0.81**
BIQI	61.37	37.75	55.35	**32.19**

shown in Fig. 2(e). From Fig. 2(f), we can see that the proposed method produces much sharper edges with abundant textures and stripes are completely removed.

To test the robustness of the proposed method to the stripes, we also carried the experiment on the image with higher stripes level in Fig. 3. The blur is still the 5×5 Gaussian blur (standard deviation $\sigma = 2.1$), and then six discontinuous stripe lines are periodically added into the blurred images in each ten lines. In Fig. 3 (c), we can find that some notably residual stripes exist in the red mark. From the results, we can conclude that the proposed method is less sensitive to the stripes than the conventional methods. The effectiveness of the proposed algorithm could be also verified with overall quantitative assessments shown in Table I and II. It can be seen that the proposed method consistently gets the best indices on different stripe noise levels.

Furthermore, to test the proposed method in handling different kinds of blur, the uniform blur and out-of-focus blur are incorporated into our experiment. Fig. 4(a) and Fig. 4(b) is the uniform blur case and out-of-focus blur case, respectively. Note that, the stripes in the Fig. 4(a) are non-periodical and with random lengths within a scan line. With the proposed method, we can clearly observe that the stripes

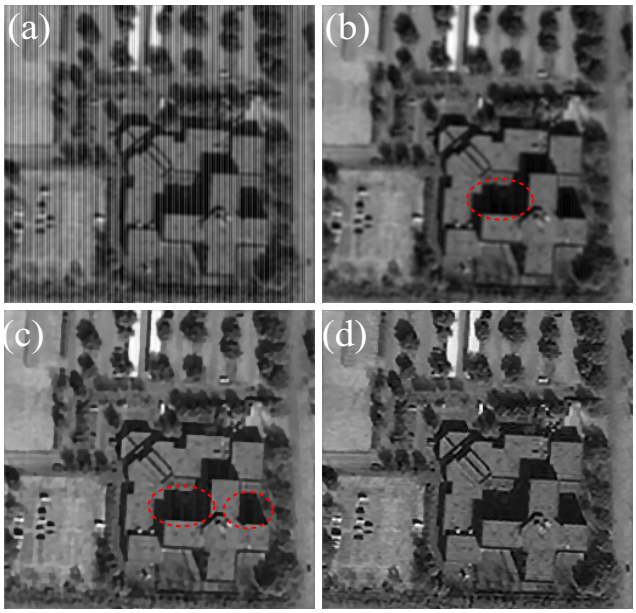

Fig. 3. Experiments with severe stripe noise. (a) Blurred image with severe stripe noise. Restored result by (b) VSNR, (c) VSNR-TV, (d) proposed method.

Table II
EVALUATION INDICES COMPARISONS UNDER SEVERE STRIPES

Index	Degraded	VSNR	VSNR-TV	Proposed
PSNR	19.90	24.16	26.55	**27.03**
UIQI	0.38	0.65	0.77	**0.80**
BIQI	72.14	32.84	42.97	**20.64**

are effectively removed. Moreover, the edges and detailed information is well recovered.

Figure 5 shows the restored results on a real hyperspectral image (band 195). The restored results demonstrate that the proposed method can efficiently remove the non-periodical stripe noise and recover images with better visual performance.

4. CONCLUSION

In this research, we proposed to couple the blind image deblurring and destriping into a unified restoration model, and demonstrate its application on remote sensing images. By combining the framelet regularization and unidirectional total variation, the proposed model could well handle different kinds of blur and stripe noise simultaneously. Both visual inspection and quantitative evaluation showed that the proposed method perform quite well in different cases and demonstrates significant improvements over that of treating them separately. Although only the remote sensing images have been investigated in this paper, the method can be applied to other sensors contaminated with similar artifact.

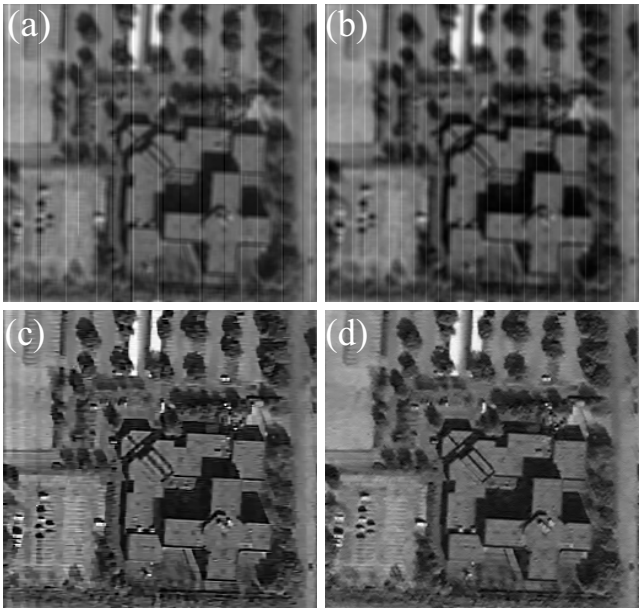

Fig. 4. Experiments with different kinds of blur. (a) Uniform blur. (b) Out-of-focus blur. (c) and (d) Restored results by the proposed method.

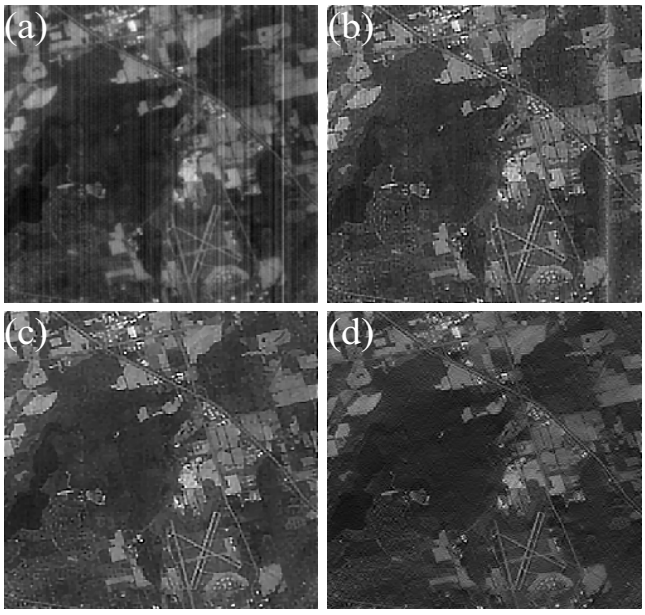

Fig. 5. Experiments with Real image. (a) Hyperspectral image (BIQI = 56.42). Restored result by (b) TV-VSNR (BIQI = 24.69), (c) VSNR-TV (BIQI = 35.39), (d) proposed method (BIQI = 24.24).

5. REFERENCES

[1] T. F. Chan and C.-K. Wong, "Total variation blind deconvolution," *IEEE Trans. Image Processing.*, vol. 7, no. 3, pp. 370-375, Mar. 1998.

[2] H. F. Shen, L. J. Du, L. P. Zhang, and W. Gong, "A blind restoration method for remote sensing images," *IEEE Geosci. Remote Sens. Lett*., vol. 9, no. 6, pp. 1137-1141, Nov. 2012.

[3] D. Kundur and D. Hatzinakos, "Blind image deconvolution," *IEEE Signal Process. Mag.*, vol. 13, no. 3, pp. 43-64, Mar. 1996.

[4] J. Cai, H. Ji, C. Liu and Z. Shen, "Framelet-based blind motion deblurring from a single image," *IEEE Trans. Image Process*., vol. 21, no. 2, pp. 562-572, Feb. 2012.

[5] H. Z. Fang, L. X. Yan, H. Liu, and Y. Chang, "Blind Poissonian images deconvolution with framelet regularization," *Opt. Lett.*, vol. 38, no. 4, pp. 389-391, Feb. 2013.

[6] P. Rakwatin, W. Takeuchi, and Y. Yasuoka, "Stripe noise reduction in MODIS data by combining histogram matching with facet filter," *IEEE Trans. Geosci. Remote Sens.*, vol. 45, no. 6, pp. 1844-1856, Jun. 2007.

[7] B. Münch, P. Trtik, F. Marone, and M. Stampanoni, "Stripe and ring artifact removal with combined wavelet-Fourier filtering," *Opt. Express.*, vol. 17, pp. 8567-8591, May. 2009.

[8] M. Bouali and S. Ladjal, "Toward optimal destriping of MODIS data using a unidirectional variational model," *IEEE Trans. Geosci. Remote Sens*., vol. 49, pp. 2924-2935, Aug. 2011.

[9] J. Fehrenbach, P. Weiss, and C. Lorenzo, "Variational algorithms to remove stationary noise: applications to microscopy imaging," *IEEE Trans. Image Process*., vol. 21, no. 10, pp. 4420-4430, Oct. 2012.

[10] T. Goldstein, and S. Osher, "The split Bregman method for L1 regularized problems," *SIAM J. Imag. Sci*., vol. 2, no. 2, pp. 323-343, May. 2009.

[11] Z. Wang and A. Bovik, "A universal image quality index," *IEEE Signal Process. Lett*., vol. 9, no. 3, pp. 81-84, Mar. 2002.

[12] A. K. Moorthy and A. C. Bovik, "A two-step framework for constructing blind image quality indices," *IEEE Signal Processing Letters.*, vol. 17, no. 5, pp. 513-516, May. 2010.